Supplemental Information

Defects in Antiviral T Cell Responses

Inflicted by Aging-Associated miR-181a Deficiency

Chulwoo Kim, Rohit R. Jadhav, Claire E. Gustafson, Megan J. Smithey, Alec J. Hirsch, Jennifer L. Uhrlaub, William H. Hildebrand, Janko Nikolich-Žugich, Cornelia M. Weyand, and Jörg J. Goronzy
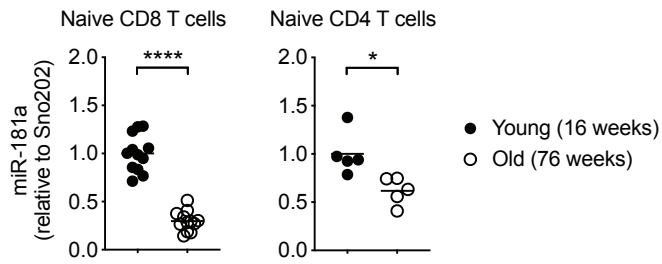
Figure S1. Mouse T cells have reduced miR-181a expression with age. Related to Figure 1.
CD62L^{+} CD44^{-} naïve CD8 and CD4 T cells were sorted from spleens of young (16 weeks) and old (76 weeks) wild-type mice; miR-181a expression was measured by quantitative RT-PCR. Results were normalized to the expression of Sno202 and are presented relative to those of cells from young mice. Data are pooled with 5-12 mice per group. Each symbol represents an individual mouse and horizontal lines indicate the mean. *p < 0.05, ****p < 0.0001 by two-tailed unpaired Student's t test.
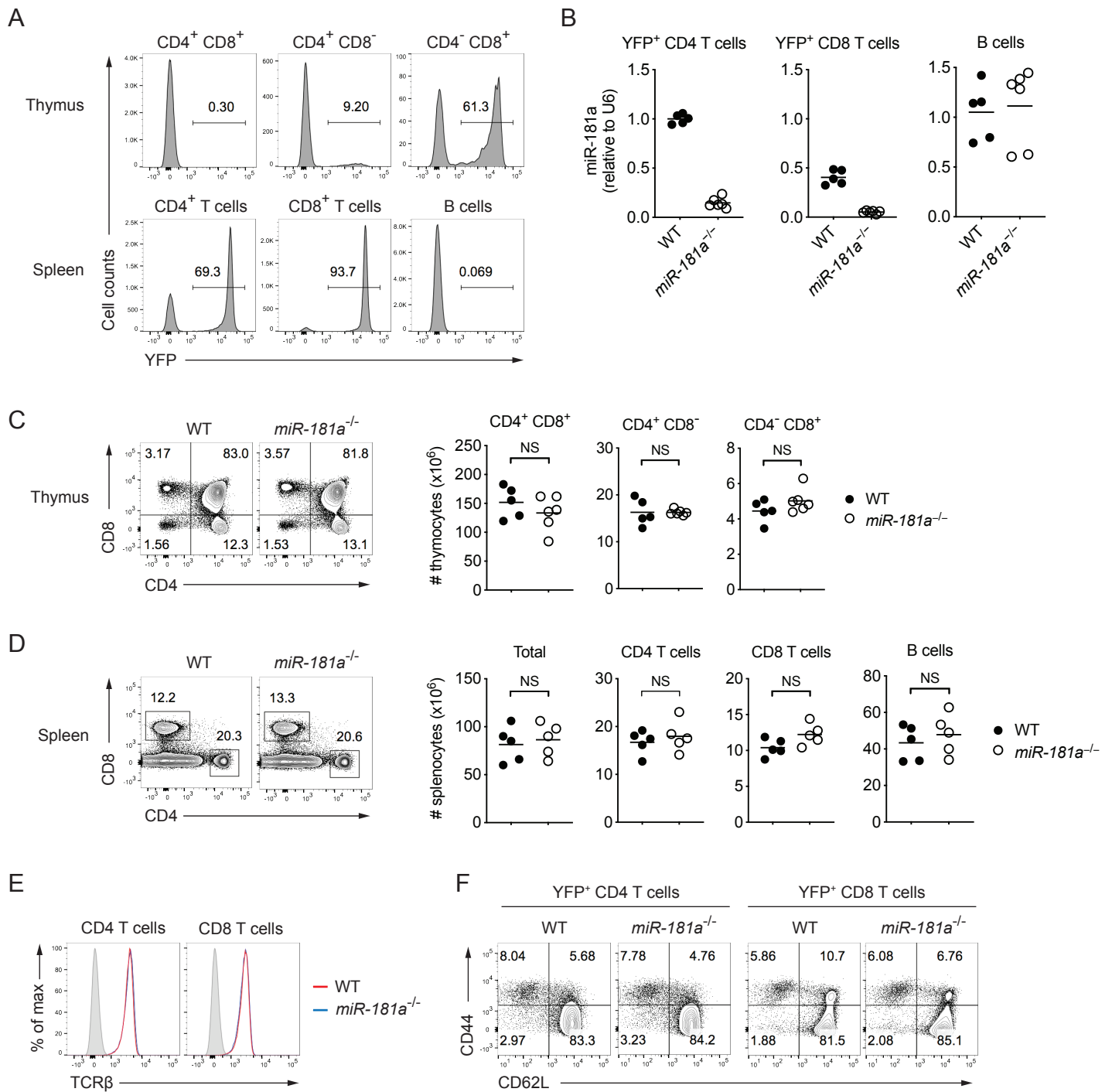
Figure S2. Generation of mice with mature T cells deficient for miR-181ab1. Related to Figure 1.
(**A**) *dLck*-Cre mice were crossed to *ROSA26*^YFP mice. Indicated cell populations in the thymus and spleen were analyzed for YFP expression, a surrogate marker for Cre-mediated gene deletion. (**B-F**) *dLck*-Cre⁺ *ROSA26*^YFP mice were crossed to *miR-181ab1*^fl/fl mice to generate *dLck*-Cre⁺ *ROSA26*^YFP *miR-181ab1*^fl/fl mice (referred to as *miR-181a*⁻/⁻ mice) and *dLck*-Cre⁺ *ROSA26*^YFP *miR-181ab1*^+/+ mice (referred to as WT mice). (**B**) YFP⁺ CD4 T cells, YFP⁺ CD8 T cells and B220⁺ B cells in the spleens of WT and *miR-181a*⁻/⁻ mice were sorted, and miR-181a expression was measured by quantitative RT-PCR. Results were normalized to the expression of U6 and are presented relative to those of YFP⁺ CD4 T cells from WT mice. (**C**) Representative flow plots of thymic T cell subsets (left) and summary data (right). (**D**) Representative flow plots of splenic CD4 and CD8 T cells (left) and summary data (right). (**E**) Representative flow plots of TCR β-chain expression and (**F**) CD44/CD62L expression by YFP⁺ CD4 and CD8 T cells in the spleen. Filled gray in (E) indicates non-T cells. Data are pooled from two independent experiments with 5-6 mice per group. Each symbol represents an individual mouse and horizontal lines indicate the mean. NS, not significant; all by two-tailed unpaired Student's t test.
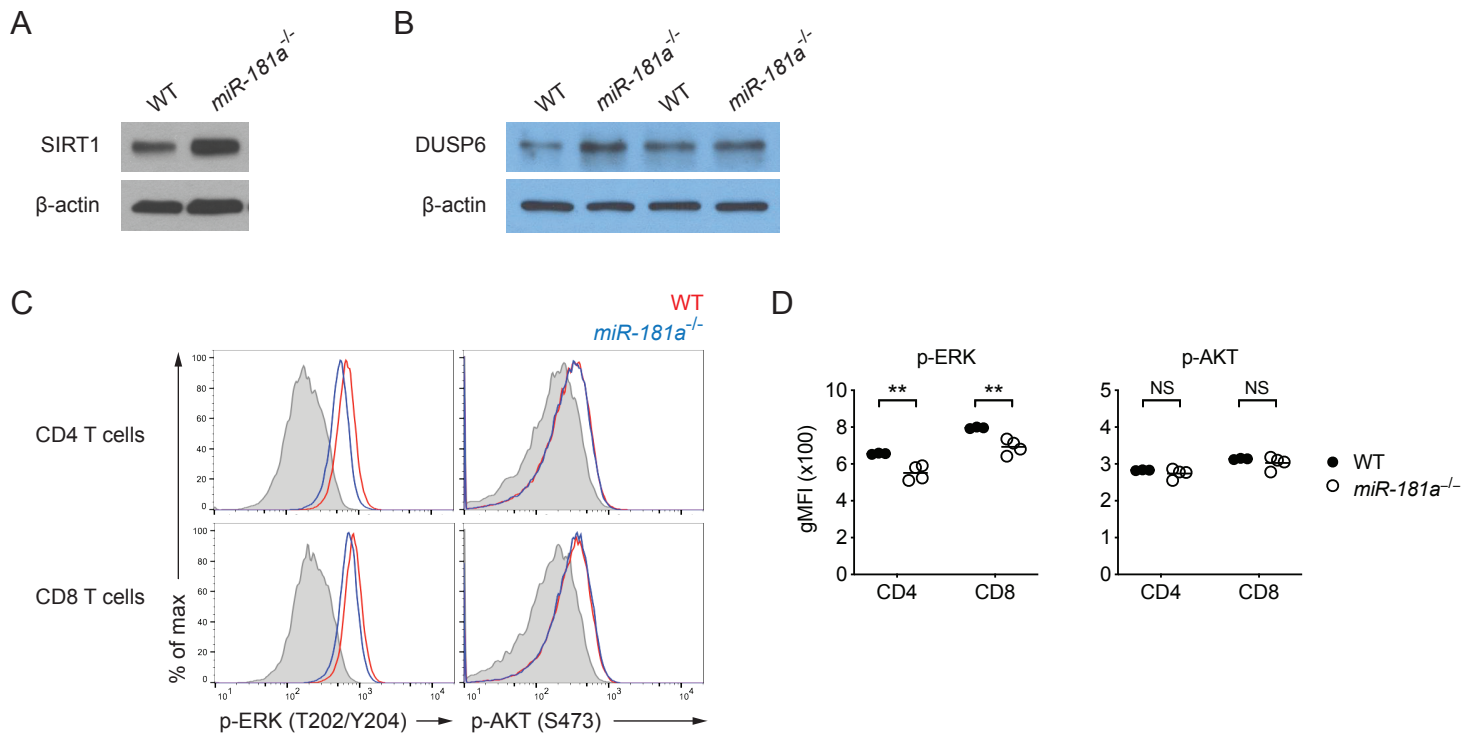
Figure S3. Expression of miR-181a target genes in miR-181a-deficient T cells. Related to Figure 1.
(**A-B**) YFP+ splenic CD4 T cells of naïve WT and *miR-181a*−/− mice were sorted. SIRT1 (**A**) and DUSP6 (**B**) expression were assessed by Western blot. (**C-D**) Total T cells isolated from the spleens of WT and *miR-181a*−/− mice were cross-linked with anti-CD3 antibody for 10 minutes. Representative histograms (**C**) and geometric MFI (**D**) of phosphorylated ERK and AKT in YFP+ CD4 and CD8 T cells are shown. Filled gray indicates unstimulated T cells. Data are representative of two independent experiments (A-B) or pooled from two independent experiments with 3-4 mice per group (C-D). Each symbol represents an individual mouse and horizontal lines indicate the mean in (D). **p < 0.01; NS, not significant; all by two-tailed unpaired Student's t test.
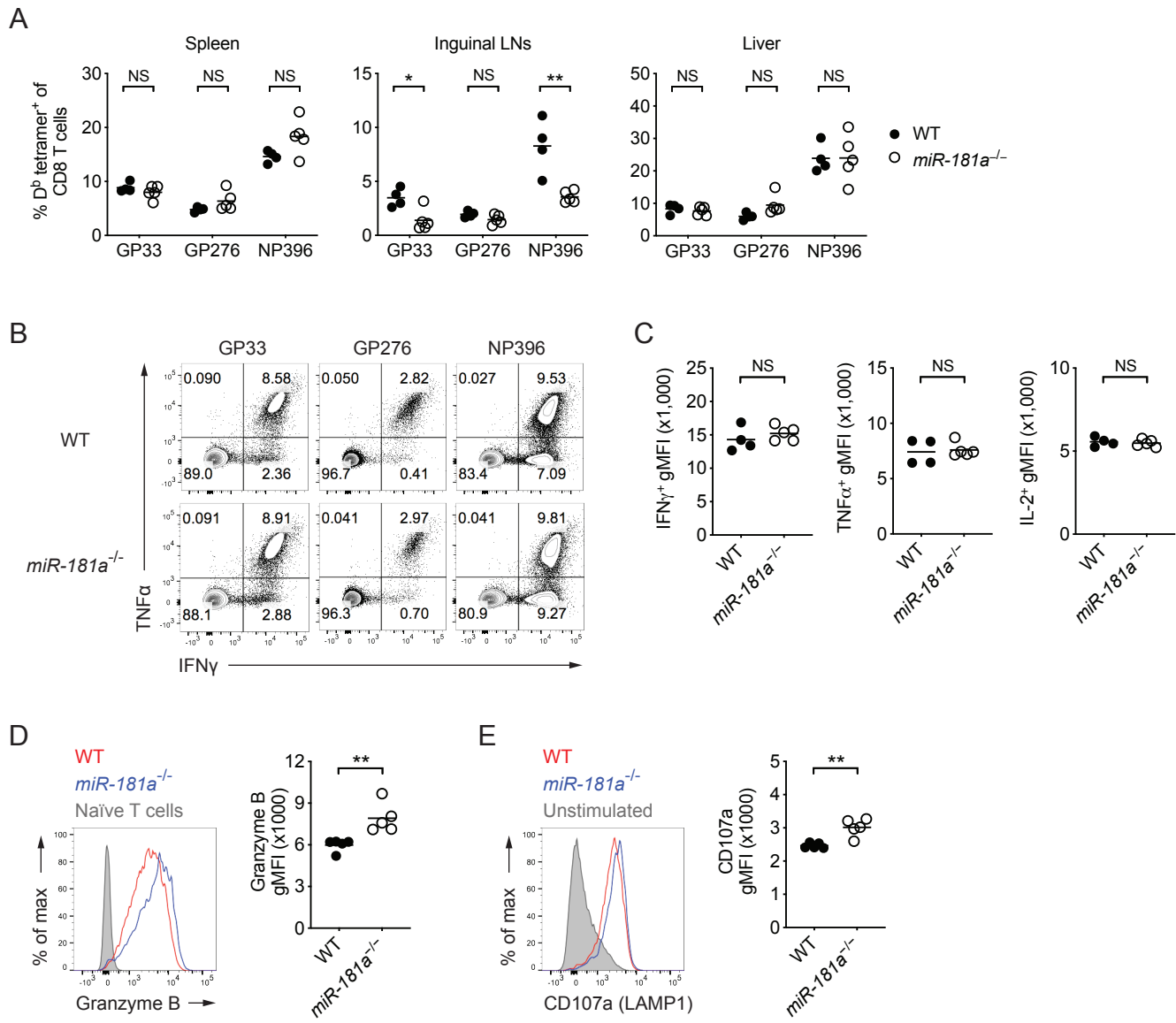
Figure S4. Functional assessment of miR-181a-deficient effector CD8 T cells. Related to Figure 1.
WT and *miR-181a*[−/−] mice were acutely infected with LCMV and analyzed on day 8. (**A**) Plots show the percent frequencies of D^b tetramer$^+$ cells for indicated epitopes among YFP$^+$ CD8 T cells in the spleen, inguinal lymph nodes and liver. (**B-E**) Splenocytes were restimulated with the indicated peptides. (**B**) Representative flow plots of IFNγ and TNFα production by YFP$^+$ CD8 T cells, (**C**) geometric MFI of IFNγ, TNFα and IL-2, (**D**) representative histogram of granzyme B production and summary graph of geometric MFI and (**E**) histogram of surface CD107a (LAMP1) and summary graph of GP33-specific CD8 T cells are shown. Data are representative of two independent experiments with 4-5 mice per group. Each symbol represents an individual mouse and horizontal lines indicate the mean. *p < 0.05, **p < 0.01; NS, not significant; all by two-tailed unpaired Student's t test.
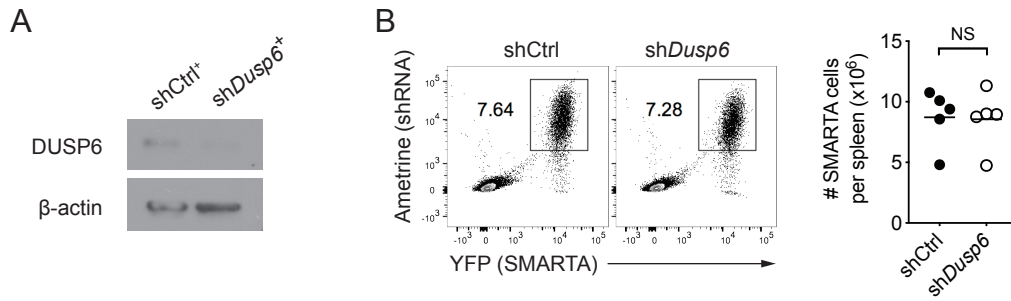
Figure S5. Dusp6 silencing of miR-181a-deficient SMARTA CD4 T cells does not rescue the defect in cell expansion. Related to Figure 2.

(**A**) miR-181a-deficient SMARTA CD4 T cells were retrovirally transduced with either shCtrl or sh*Dusp6*. DUSP6 and β-actin expression were assessed on sorted shCtrl⁺ and sh*Dusp6*⁺ cells (Ametrine⁺ YFP⁺ CD4⁺) by Western blot. (**B**) shCtrl⁺ and sh*Dusp6*⁺ miR-181a-deficient SMARTA cells were sorted and adoptively transferred into B6 hosts, followed by LCMV infection four days later. Representative flow plots of shRNA⁺ SMARTA cell frequency among total CD4 T cells on day 8 (left) and summary graph of the total number of shRNA⁺ SMARTA cells in the spleen are shown. Data are from one experiment with 5 mice per group. Each symbol represents an individual mouse and horizontal lines indicate the mean. NS, not significant by two-tailed unpaired Student's t test.
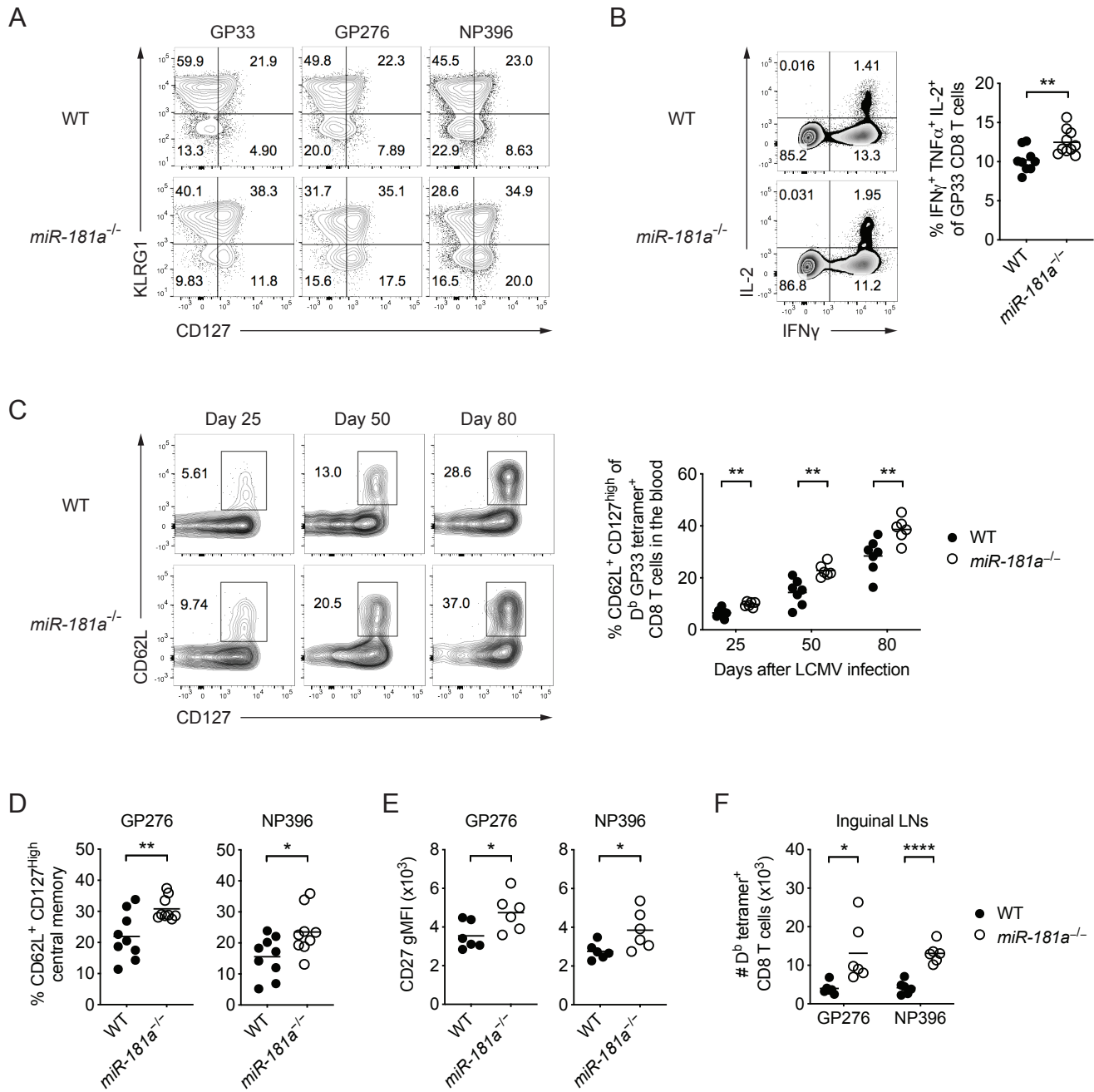
Figure S6. miR-181a is required for the generation of effector memory CD8 T cells. Related to Figure 4.
WT and *miR-181a⁻/⁻* mice were infected with LCMV. (**A**) Representative flow plots of KLRG1 and CD127 expression by D^b tetramer⁺ YFP⁺ CD8 T cells for indicated epitopes are shown on day 8. (**B**) Representative flow plots of IFNγ and IL-2 production (left) and summary data of the proportion of cells co-producing IFNγ, TNFα and IL-2 (right) by D^b GP33 tetramer⁺ YFP⁺ CD8 T cells on day 8. (**C**) Representative flow plots of CD62L and CD127 expression (left) and summary data of CD62L⁺ CD127^high central memory cell frequencies (right) among D^b GP33 tetramer⁺ YFP⁺ CD8 T cells in the blood at indicated time points after LCMV infection. (**D-F**) WT and *miR-181a⁻/⁻* mice were infected with LCMV, and memory CD8 T cells were analyzed on day 90. Plots show the relative frequency of CD62L⁺ CD127^high central memory cells (**D**) and geometric MFI of CD27 expression (**E**) of D^b tetramer⁺ memory CD8 T cells for indicated epitopes in the spleen. (**F**) Plots show the numbers of D^b tetramer⁺ memory CD8 T cells for indicated epitopes in lymph nodes. Data are representative of three independent experiments with 4-5 mice per group (A) or pooled from 2-3 independent experiments with 6-10 mice per group (B-F). Each symbol represents an individual mouse and horizontal lines indicate the mean. *p < 0.05, **p < 0.01, ****p < 0.0001; all by two-tailed unpaired Student's t test.
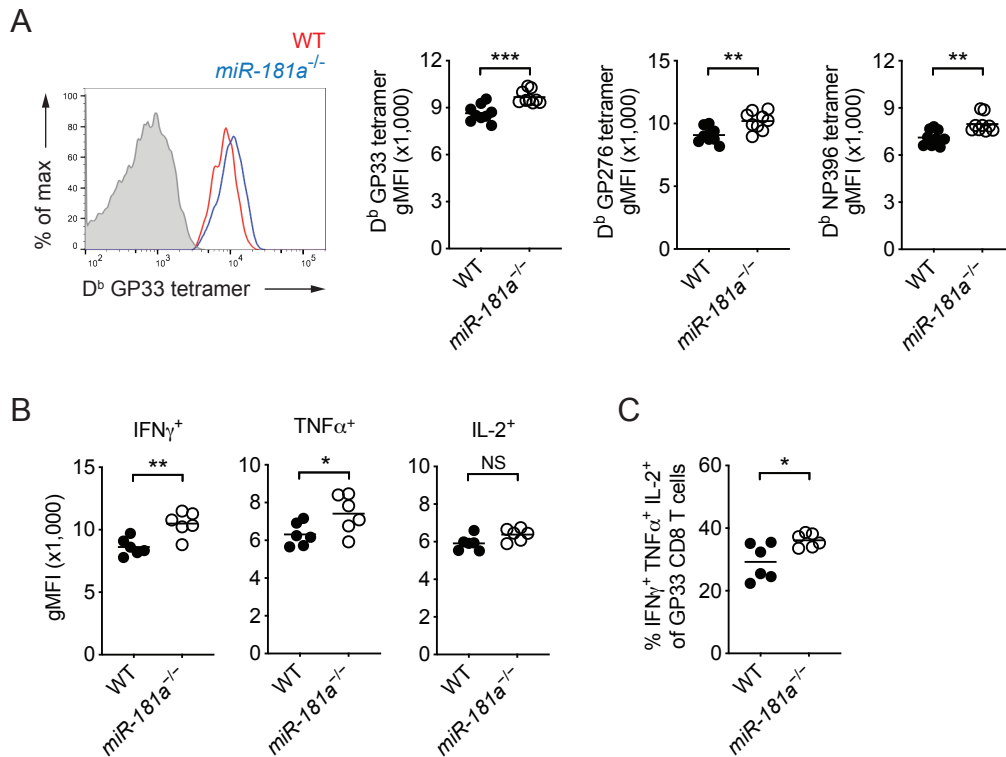
Figure S7. Characterization of miR-181-deficient memory CD8 T cells. Related to Figure 4.
WT and *miR-181a*$^{-/-}$ mice were infected with LCMV, and their spleens were harvested on day 85. (**A**) Representative histogram of tetramer binding intensity of D^b GP33 tetramer$^+$ YFP$^+$ CD8 T cells (left) and dot plots of geometric tetramer MFI for indicated epitopes (right) are shown. Filled gray in histogram indicates naïve CD8 T cells. Dot plots show geometric MFI of indicated cytokines (**B**) and the proportion of cells co-producing IFNγ, TNFα and IL-2 (**C**) by GP33-specific YFP$^+$ CD8 T cells. Data are pooled from two independent experiments with 6 mice per group. Each symbol represents an individual mouse, and horizontal lines indicate the mean. Statistical significance was determined by two-tailed unpaired Student's t test. *P < 0.05; **P < 0.01; ***P < 0.001; NS, not significant.